July 1994

Ozone Heating and the Destabilization of Traveling Waves During Summer

Terrence R. Nathan
University of California - Davis

Eugene Cordero
University of California - Davis, eugene.cordero@sjsu.edu

Long Li
University of California - Davis

Recommended Citation

Terrence R. Nathan, Eugene Cordero, and Long Li. "Ozone Heating and the Destabilization of Traveling Waves During Summer" *Geophysical Research Letters* (1994): 1531-1534. doi:10.1029/94GL01108

GEOPHYSICAL RESEARCH LETTERS, VOL. 21, NO. 14, PAGES 1531-1534, JULY 1, 1994

Ozone heating and the destabilization of traveling waves during summer

Terrence R. Nathan, Eugene C. Cordero, and Long Li

Atmospheric Science Program
University of California, Davis, CA 95616

Abstract. The effects of ozone heating on the linear stability of lower stratospheric traveling waves of the summertime, extratropical circulation are examined. Based on coupled equations for the quasigeostrophic potential vorticity and ozone volume mixing ratio, it is shown that the diabatic heating arising from ozone advection can offset the damping due to Newtonian cooling, leading to wave amplification and significant changes in the structure and zonally rectified fluxes of the wave fields in both the lower stratosphere *and* troposphere. The vertical profile of the zonal mean wind plays a crucial role in determining whether the ozone heating destabilizes eastward and/or westward traveling disturbances.

Introduction

Traveling waves having signatures in the troposphere and lower stratosphere are an integral part of the summertime, extratropical circulation of the Northern and Southern Hemispheres (Muench 1968; White 1982; Yu et al. 1984; Randel and Stanford 1985). Observations show these waves to be of two general types: large-scale, westward traveling disturbances and medium-scale, eastward traveling disturbances. The former have been identified as Rossby waves (Muench 1968), though the origin and processes that affect their life cycles remain unclear. The medium-scale, eastward traveling disturbances generally have baroclinic structures and are attributed to the instability of the zonal mean current (Yu et al. 1984). Because both wave types have significant amplitude in the lower stratosphere, they not only play an important role in ozone transport (Schoeberl and Kruger 1983), but may themselves be affected by ozone heating (Nathan and Li 1991).

Evidence that ozone-dynamics interactions in the lower stratosphere during summer may lead to changes in the free wave structure and transport properties of the lower stratosphere and troposphere was presented by Nathan and Li (1991; hereafter NL). Using a mechanistic model they demonstrated, for a *climatological* summer basic state, that the diabatic heating due to ozone-dynamics interaction destabilizes eastward and westward-propagating modes that are otherwise damped by Newtonian cooling. These waves were shown to coexist with baroclinically unstable waves having similar spatial scales and growth rates.

The summer climatological basic state considered by NL has several interesting features. Most notably, for the waves that are most strongly affected by ozone-dynamics interaction, the zero wind line, the change in sign of the basic state potential vorticity gradient, and the maximum in the northward gradient of basic state ozone approximately coincide at about 18 km. To what extent NL's findings can be attributed to the unique relationship among these background flow characteristics remains unclear. Therefore, to test the robustness of NL's results, and to more fully understand the role of ozone-dynamics interaction in affecting the growth, propagation, and transport properties of the traveling waves of the summertime, midlatitude circulation, we extend their study by considering several *instantaneous* distributions of the basic state zonal wind.

Paper number 94GL01108
0094-8534/94/94GL-01108$03.00

Model and Basic States

The model used here is essentially that of Nathan (1989) and NL. Briefly, we consider a baroclinic, quasigeostrophic flow on a periodic β-plane centered at 45°N. The flow is linearized about a steady, zonally averaged basic state that varies only in the vertical. The linear response of this model atmosphere to Newtonian cooling and ozone heating is described by coupled equations for the quasigeostrophic potential vorticity and ozone volume mixing ratio. The variables are the geostrophic streamfunction, ϕ', vertical velocity, w′, and ozone volume mixing ratio, γ'. We note that the vertical velocity is obtained from the quasigeostrophic thermodynamic equation; the temperature and wind fields can be obtained from knowledge of ϕ'. The perturbation fields are chosen of the form

$$(\phi',w') = Re\{[\phi(z;\sigma),w(z;\sigma)]\exp[z/2H+i(k^*x-\sigma t)]\}, \quad \text{(1a)}$$

$$\gamma' = Re[\gamma(z;\sigma)\exp i(k^*x-\sigma t)], \quad \text{(1b)}$$

where the streamfunction and vertical velocity vertical structures are density weighted. Here $\sigma = \sigma_r + i\sigma_i$ is the (complex) frequency, $H = 7$ km is the density scale height, and $k^* = k(a_e\cos\theta)^{-1}$, where $k = 1,2,3\cdots$ is the *quantized* zonal wavenumber, a_e is Earth's radius and θ is latitude. The dependence of the vertical structures $\phi(z;\sigma)$, $w(z;\sigma)$, and $\gamma(z;\sigma)$ on the eigenvalue σ is made explicit for reasons that will become apparent in the subsequent analysis.

As in NL, the solutions for the dependent variables were obtained numerically using second-order finite differences on a staggered uniform grid in which the vertical structures $\phi(z;\sigma)$ and $[w(z;\sigma), \gamma(z;\sigma)]$ were evaluated at odd and even levels, respectively. The resulting set of algebraic equations were cast in the form of a matrix-eigenvalue problem. To insure that our solutions were physically meaningful and not an artifact of vertical resolution or the location of the upper boundary, the eigenvalue problem was solved numerically for several different grid spacings, Δz, and upper boundary heights, z_t. For the results to be presented here, $\Delta z = 1$ km and $z_t = 50$ km proved sufficient in resolving the dominant instabilities.

NL carried out calculations based on a climatological distribution of wind, temperature and ozone characteristic of each season. The summer distributions, which are depicted in Figs. 1-4 in NL, were constructed from observational data of the Northern Hemisphere for July. Here the basic state temperature and ozone distributions remain as in NL, but we consider instantaneous zonal wind configurations of the form

$$\bar{u}(z) = \bar{u}_c(z) + U\cosh\frac{(z-z_0)}{D}, \quad \text{(2)}$$

where $\bar{u}_c(z)$ is the summer climatological wind profile (hereafter profile C) used by NL. Zonal mean perturbations to that basic

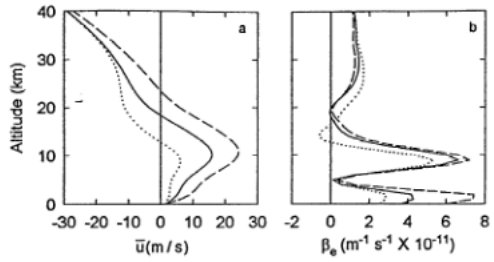

Figure. 1. (a) The zonal mean wind distributions corresponding to eq. 2. Profile 1 (dashed), profile 2 (dotted), and the climatological profile (profile C; solid). For profile 1 (profile 2), the parameters in eq. 2 are: U = 10 m/s (-14 m/s); z_0 = 18 km (15 km); and D = 10 km (5 km). (b) The basic state potential vorticity gradient, β_e, corresponding to profile 1 (dashed), profile 2 (dotted), and profile C (solid).

state are controlled by the last term on the right-hand side of (2), where U measures the strength of the perturbation, z_0 determines the level at which the mean wind perturbation is centered, and D determines its depth. Numerical calculations have been carried out for a variety of basic state wind profiles. Shown in Fig. 1a are two instantaneous wind profiles which yield solutions that typify the traveling wave response to changes in the mean wind. The climatological wind used by NL is also shown for comparison. The northward gradient of basic state potential vorticity, β_e, corresponding to the wind profiles shown in Fig. 1a are displayed in Fig. 1b.

Zonal mean wind profile 1 has a maximum wind speed of ~25 m/s and is characterized by a transition from westerlies to easterlies at ~23 km, which is ~5 km higher than that for profile C and ~10 km higher than profile 2. Because vertical wave propagation is generally favored when the background winds are weak and westerly (Charney and Drazin 1961), we can anticipate that the elevated zero wind line of profile 1 will yield disturbances that penetrate higher into the stratosphere than the other wind distributions shown in Fig. 1. For all three profiles shown in Fig. 1a, the meridional temperature gradient and thus vertical wind shear are non-zero at the surface, thus satisfying the necessary condition for baroclinic instability of inviscid, adiabatic flow (Charney and Stern 1962).

Results

NL have shown that for profile C three waves emerge that have particular physical significance. One is a baroclinically unstable wave whose structure is consistent with the medium scale baroclinic wave structures observed by Randel and Stanford (1985) for Southern Hemisphere summer. This wave is only slightly affected by ozone heating (OH). The other two waves, representing eastward and westward traveling modes, are damped when Newtonian cooling (NC) is the sole diabatic process. When NC and OH are considered in combination, these waves amplify with e-folding times comparable to that of the baroclinic wave. The e-folding times and periods of all three waves as a function of zonal wavenumber are summarized in Table 1 for the climatological basic state (profile C) as well as for zonal mean wind profiles 1 and 2.

For profile 1 only two of the three waves obtained for profile C remain: a baroclinically unstable wave and an eastward-propagating wave that is destabilized by OH. The e-folding times and periods of the k = 3-4 baroclinic waves are a factor of 3 to 4 times smaller than baroclinic waves of profile C, and show little variation with changes in zonal wave scale (see Table 1). These smaller e-folding times and periods, which are insensitive to the effects of OH, are due, respectively, to the increased tropospheric wind shear and increased mean wind of profile 1. The vertical structure of the baroclinically unstable waves are similar for profile 1 and for profile C. The westward tilt with height of the waves is maximized in the lower to middle troposphere, yielding poleward fluxes of heat and potential vorticity that peak near the surface (not shown).

The influence of OH on the ozone induced eastward-propagating waves is pronounced. For example, in the absence of OH, the k = 3 wave has an e-folding damping time of -20.1 d. However, when OH is included, the wave amplifies with an e-folding time of 31 d. In contrast to the baroclinically unstable wave, the e-folding times of the eastward-propagating waves are much less sensitive to changes in the mean wind distribution. For instance, the k = 2-3 waves all have e-folding times in the 30-40 d range for all three wind profiles (see Table 1). The periods of these waves, however, are sensitive to the mean wind distribution, being about an order of magnitude shorter for profile 1 than for profile C.

Figure 2 displays, for profile 1, the normalized vertical structure of the k = 4 eastward-propagating wave for NC alone (left column) and for NC and OH combined (right column). Comparison of Figs. 2a and 2b shows a significant change in wave structure resulting from OH. When NC is the sole diabatic process, the streamfunction amplitude is maximized at ~10 km, with two secondary maxima of about equal amplitude located at the surface and ~20 km. The ozone amplitude is sharply peaked at ~20 km, and from ~18 km and ~21 km slowly tapers to about zero at ~10 km and ~40 km, respectively. When NC and OH are considered in combination, the streamfunction amplitude is maximized at ~20 km, which coincides with the maximum in the ozone amplitude. A particularly striking feature is the influence of the OH on the wave structure in the troposphere. For example, the local minimum in streamfunction amplitude modulus at ~3 km for the NC case is eliminated when OH is taken into account (compare Figs. 2a and 2b). Moreover, the phase of the streamfunction, which decreases by 180° from the surface to ~4 km for the NC case, montonically increases from ~0° at the surface to ~90° at ~10 km under the combined influence of NC and OH. This 90° increase in phase corresponds to a westward tilt with height and thus a net poleward heat

Table 1. Below is listed the (period, e-folding time) in days for the most unstable baroclinic wave and the most unstable ozone induced waves that arise for the basic states shown in Fig. 1. The dashed lines indicate that the wave is damped.

Wave type	Zonal Wavenumber, k				
	1	2	3	4	5
			Climatological Mean Wind		
Eastward-propagating	(353,75)	(165,36)	(108,32)	(80,350	(64,44)
Westward-propagating	(-94,90)	(-48,39)	(-32,31)	(-24,31)	(-16,60)
Baroclinically unstable	———	———	(27,44)	(20,31)	(15,45)
			Zonal Mean Wind Profile 1		
Eastward-propagating	(54,79)	(27,39)	(18,33)	(13,36)	16,52)
Baroclinically unstable	———	(19,16)	(13,11)	(9,6,10)	———
			Zonal Mean Profile 2		
Westward-propagating	(-124,85)	(-62,38)	(-42,31)	(-8,32)	(-6,34)

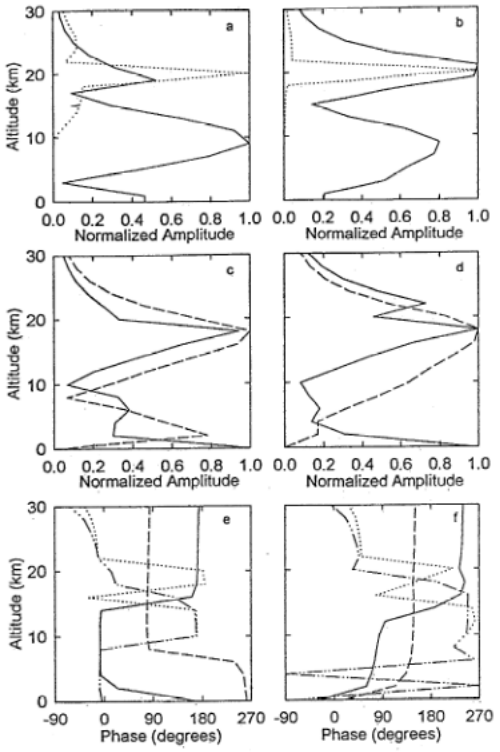

Figure 2. The effects of Newtonian cooling (left column) and Newtonian cooling and ozone heating combined (right column) for the $k = 4$ wave vertical structure of profile 1. The moduli of (a), (b) streamfunction $|\phi|$ (solid), ozone $|\gamma|$ (dotted), (c), (d) vertical velocity $|w|$ (dashed) and temperature $|T|$ (solid). (e), (f) Vertical phase structure of the streamfunction (solid), ozone (dotted), vertical velocity (dashed), and temperature (dashed-dotted). Because the perturbation ozone amplitude virtually vanishes in the troposphere, its phase is not plotted below 10 km. For clarity, the figures are only shown to 30 km, although all calculations were carried out to 50 km.

transport (see Fig. 3b). Similar changes in tropospheric phasing are also evident for the vertical motion field.

To understand how OH in the stratosphere can influence wave structures in the troposphere, it is important to recognize that normal mode wave structures, like the ones considered here [see eq. (1)], depend on the *global* growth characteristic of the wave fields, as measured by the normal mode growth rates, σ_i. Thus changes in σ_i that are produced locally may have a strong influence on the wave structure far from the source of the instability, which here arises primarily from the OH in the lower stratosphere.

The ozone-streamfunction phase relationships shown in Figs 2e and 2f can be qualitatively understood by examining the ozone continuity equation. Using the fact that ozone is under dynamical control in the lower stratosphere and that our numerical calculations show that vertical ozone advection is much smaller than meridional ozone advection, the ozone continuity equation [eq. (2.4) in NL] can be approximated by

$$\gamma' \approx -k^* \left[\frac{i\sigma_i + \omega}{\sigma_i^2 + \omega^2}\right] \frac{\partial \bar{\gamma}}{\partial y} \phi', \tag{3}$$

where σ_i is the growth rate and $\omega = (\bar{u}k^* - \sigma_r)$ is the Doppler shifted frequency. Thus the ozone-streamfunction phase difference depends on the relative importance of wave transience and wave propagation, measured, respectively, by σ_i and ω. If the latter dominates, γ' and ϕ' are in phase when $\partial\bar{\gamma}/\partial y < 0$ and 180^0 out of phase when $\partial\bar{\gamma}/\partial y > 0$. If wave transience dominates, γ' and ϕ' are $\pm 90^0$ out of phase, the sign of which depends on whether the wave is growing ($\sigma_i > 0$) or decaying ($\sigma_i < 0$) and whether the meridional ozone gradient is positive ($\partial\bar{\gamma}/\partial y < 0$) or negative ($\partial\bar{\gamma}/\partial y < 0$). The ozone-streamfunction phase relationship shown in Fig. 2 is consistent with the interpretation provided by (3). For example, calculations show that $\omega \approx 0$ at $\sim$20.5 km, which coincides with the level where the streamfunction and ozone fields are $\sim 90^0$ out of phase.

Based on the ozone induced changes in vertical phasing depicted in Fig. 2d, we can also anticipate similar changes in the zonal mean eddy fluxes. For instance, as comparison of Figs. 3a and 3b shows, OH reverses the eddy fluxes in the troposphere.

The reversal in ozone transports shown in Figs. 3c and 3d are directly related to the change in wave transience arising from the OH. To illustrate this, consider the following expression for the zonally averaged poleward transport of ozone,

$$\overline{v'\gamma'} = -\frac{\sigma_i}{\sigma_i^2 + \omega^2} \frac{\partial \bar{\gamma}}{\partial y} |v|^2, \tag{4}$$

which has been obtained by multiplying the ozone continuity equation [eq. (2.4) in NL] by the meridional velocity v', zonally averaging, and applying the approximations that were used in deriving (3). Equation (4) shows that poleward ozone transport hinges on either wave growth or decay, and may become locally large at the critical level, i.e., where $\omega \to 0$. In Fig. 3d, for example, the ozone transports are maximized where $\omega \approx 0$, i.e., at $\sim$20 km.

For profile 2 an ozone-induced, westward-propagating wave is the sole amplifying wave. The absence of baroclinically unstable waves for this wind profile is attributed to the relatively weak tropospheric wind shear, which is about a factor of four less than that of profile 1. In contrast to the wave destabilized by OH shown in Fig. 2, the amplitude moduli of the westward-propagating wave of profile 2 are much less affected by the OH (compare Figs. 2a-2d with Figs. 3a-3d) and decrease more rapidly above their lower stratospheric maximum. This latter feature is due to the greater vertical trapping associated with the lower zero wind line of profile 2. Like the wave discussed in Fig. 2, however, the OH yields *e*-folding times on the order of 30-40 d (see Table 1) and results in large changes in the vertical phasing of the wave in both the troposphere and stratosphere (see Figs. 4e and 4f). These ozone induced phase changes yield zonally rectified eddy transports that are primarily confined to the lower stratosphere (see Fig. 5b).

Finally, we note that because the traveling waves of the summertime, midlatitude circulation are vertically trapped, being

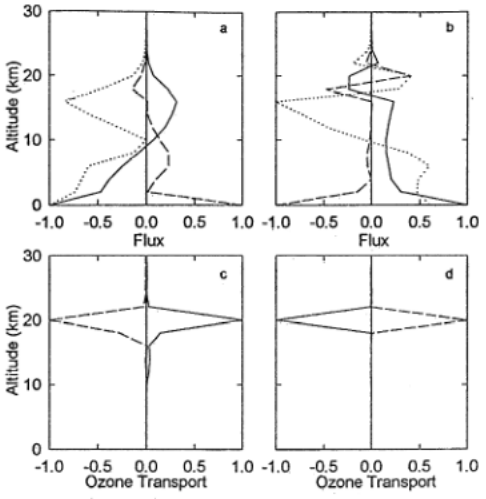

Figure 3. Zonally averaged wave fluxes corresponding to the wave structure shown in Fig. 2. (a), (b) Poleward heat flux, $\rho v \varphi_z$ (solid), vertical heat flux (dotted), $\rho w \varphi_z$, and potential vorticity flux, $\rho v q$ (dashed), where q' is the perturbation potential vorticity. (c), (d) Poleward ozone transport, (solid), and vertical ozone transport, $\rho v \gamma$ (dashed).

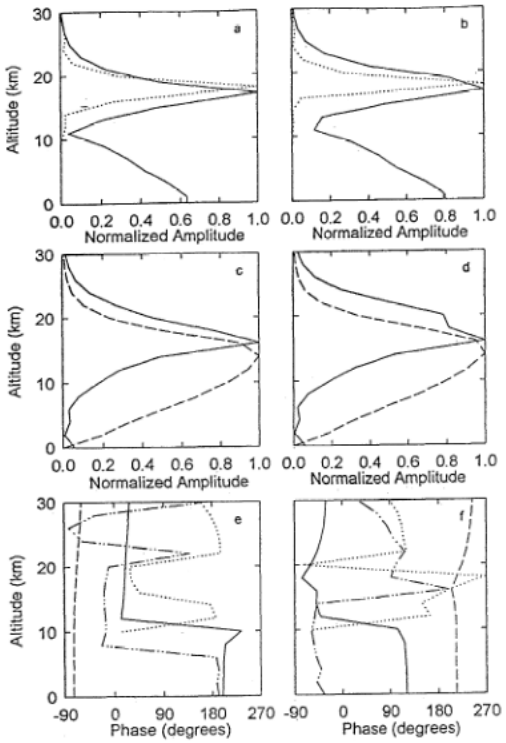

Figure 4. As in Fig. 2, but for zonal mean wind profile 2.

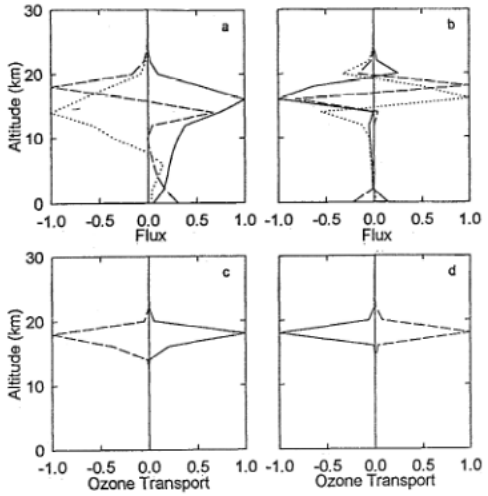

Figure 5. As in Fig. 3, but for zonal wind profile 2.

confined to the lower stratosphere where the advective time scale dominates over the photochemical time scale, the diabatic heating is due primarily to the advection of basic state ozone by the waves. Our calculations show that meridional ozone advection dominates over vertical advection, the latter having less than a 5% effect on *e*-folding times.

Concluding Remarks

The destabilizing influence of ozone heating on the traveling waves of midlatitude summer has been investigated for several different zonal wind profiles representative of that season. The results show that the heating due to ozone-dynamics coupling dominates over the damping effects of Newtonian cooling, leading to wave amplification and dramatic changes in wave structure in both the lower stratosphere and troposphere. For a climatological wind profile, both eastward and westward traveling disturbances are destabilized by ozone; their growth rates are comparable to the baroclinically unstable waves. For sufficiently strong tropospheric wind shears, the westward traveling wave is damped; the eastward traveling ozone wave remains, though its growth rate is much less than that of the baroclinic waves. For sufficiently weak tropospheric wind shears, the baroclinically unstable waves are eliminated; only westward traveling waves that are destabilized by ozone remain. The *e*-folding times of the waves destabilized by ozone are generally much less sensitive to changes in the vertical wind shear than the baroclinic waves.

The meridional and vertical transport of ozone by the waves destabilized by OH are sharply confined to the lower stratosphere. These transports have been shown to depend on the relative importance of wave transience and wave propagation, both of which are strongly influenced by coupling between the ozone and dynamics fields.

Perhaps our most important result is that the vertical wind profile can have a strong effect on the destabilizing influence of OH and corresponding tropospheric wave fluxes. By altering the global growth characteristics of the waves, as measured by the normal mode growth rates, the OH in the lower stratosphere was shown to influence the wave structures far from the source of the instability. These results underscore the importance of the combined influence of the vertical wind profile and OH in affecting wave transience and wave dissipation in the stratosphere. Although our findings are based on an idealized model of the middle latitude circulation during summer, they strongly suggest that in addition to baroclinic instability, OH may play a more important role in the generation of traveling waves than previously thought.

Acknowledgments. The authors thank Matt Pyle for assisting in the numerical calculations. The authors also thank Bob Echols and Cindy Shellito for providing comments on the manuscript. This work was supported by NASA grant NAG8-871, NASA training grant NGT-30153, and the University of California Institute for Collaborative Research (INCOR). Support has also been provided for Eugene Cordero through NASA's Global Change Fellowship Program.

References

Charney, J., and P. Drazin, Propagation of planetary scale disturbances from the lower into the upper atmosphere, *J. Geophys. Res.*, **66**, 83-109, 1961.

Charney, J., and M. Stern, On the stability of internal baroclinic jets in a rotating atmosphere, *J. Atmos. Sci.*, **19**, 159-172, 1962.

Muench, H. S., Large-scale disturbances in the summertime stratosphere, *J. Atmos. Sci.*, **25**, 1108-1115, 1968.

Nathan, T. R., On the role of ozone in the stability of Rossby normal modes, *J. Atmos. Sci.*, **46**, 2094-2100, 1989.

Nathan, T. R., and L. Li, Linear stability of free planetary waves in the presence of radiative-photochemical feedbacks, *J. Atmos. Sci*, **48**, 1837-1855, 1991.

Randel, W. J., and J. L. Stanford, An observational study of medium scale waves in the Southern Hemisphere summer, *J. Atmos. Sci.*, **42**, 1172-1188, 1985.

Schoeberl, M. R., and A. J. Krueger, Medium scale disturbances in total ozone during Southern Hemisphere summer, *Bull. Amer. Met. Soc.*, **64**, 1358-1365, 1983.

White, G. H., An observational study of the Northern Hemi sphere extratropical summertime general circulation, *J. Atmos. Sci.*, **39**, 24-40, 1982.

Yu, W.-B., J. L. Stanford, and R. L. Russell, Some interhemi spheric comparisons of medium scale waves in the lower stratosphere, *J. Atmos. Sci.*, **41**, 2084-2088, 1984.

(Received March 3, 1994; Revised April 19, 1994; Accepted April 22, 1994.)